Estimates of Himalayan Tahr (*Hemitragus jemlahicus*) Abundance in New Zealand

Results from Aerial Surveys

D.S.L. Ramsey and D.M. Forsyth

September 2019

Arthur Rylah Institute for Environmental Research
Unpublished Client Report

Arthur Rylah Institute for Environmental Research
Department of Environment, Land, Water and Planning
PO Box 137
Heidelberg, Victoria 3084
Phone (03) 9450 8600
Website: www.ari.vic.gov.au

Citation: Ramsey, D.S.L., and Forsyth. D.M. (2019). Estimates of Himalayan tahr (*Hemitragus jemlahicus*) abundance in New Zealand: Results from aerial surveys. Unpublished Client Report for the New Zealand Department of Conservation. Arthur Rylah Institute for Environmental Research, Department of Environment, Land, Water and Planning, Heidelberg, Victoria.

Front cover photo: Tahr aerial surveys in the Southern Alps, New Zealand (Mike Perry).

Estimates of Himalayan Tahr (*Hemitragus jemlahicus*) abundance in New Zealand

Results from aerial surveys

[1]D.S.L. Ramsey and [2]D.M. Forsyth

[1]Arthur Rylah Institute for Environmental Research
123 Brown Street, Heidelberg, Victoria 3084

[2]Vertebrate Pest Research Unit, NSW Department of Primary Industries
1447 Forest Road, Orange, NSW, 2800

In partnership with

Department of Conservation
Te Papa Atawhai

Arthur Rylah Institute for Environmental Research
Department of Environment, Land, Water and Planning
Heidelberg, Victoria

Acknowledgements

We acknowledge the Department of Conservation staff (particularly Pete Thomas and Kat Manno) and helicopter pilots who conducted the field surveys. Meredith McKay, Benno Kappers and Richard Earl assembled the aerial survey data and analysed the DEM and LCDB layers used to estimate the surface area and habitat composition of monitoring plots. Funding for this project was provided by the Biodiversity Group, Department of Conservation, New Zealand.

Contents

1 Summary

Context:

The Himalayan Tahr Control Plan (Department of Conservation 1993) defines intervention densities in terms of number of tahr per km^2 in each of seven management units (range: <1 to 2.5 tahr per km^2) and two exclusion zones (0 per km^2) and sets a limit on total population abundance to no more than 10,000 animals. Prior to this study, insufficient information existed to determine whether tahr numbers in each management unit and exclusion zone exceeded these intervention densities or whether the total population abundance exceeded the limit.

Aims:

To estimate the total abundance of Himalayan tahr on Public Conservation Land (PCL) and then use this to derive estimates separately for the seven management units and two exclusion zones in the Southern Alps of New Zealand.

Methods:

Aerial surveys to count tahr and other ungulates were conducted on three occasions at 117 plots (2 x 2 km) located on PCL from 2016 to 2019. The repeat counts of tahr were used to estimate abundance, corrected for imperfect detection, using an *N*-mixture model for open populations (Dail & Madsen 2011). Design-based, finite sampling methods were then used to estimate the total abundance of tahr on PCL as well as for each management unit and exclusion zone (Skalski 1994). This work updates a previous analysis that was based on data collected up to 2018 (Ramsey & Forsyth 2018).

Results:

- The total abundance of tahr on PCL for the period 2016 – 2019 was estimated to be 34,478 individuals (95% confidence interval; 26,522 – 44,821).
- Tahr abundances were highest in management unit 3 (approximately 8,600 tahr), and were lowest in management unit 7 (169 tahr) and the two exclusions zones (approximately 30 – 50 tahr).
- Average tahr density over the three years of sampling was highest in management unit 5 (10.8 tahr/km^2) and lowest in exclusion zone 2 (0.02 tahr/km^2).

Conclusions and implications:

- Average tahr densities exceeded the intervention densities specified in the Himalayan Tahr Control Plan in all management units and in both exclusion zones, with the exception of management unit 7.
- The estimated total population abundance of tahr on PCL clearly exceeds the limit of 10,000 animals. Moreover, the lower 95% confidence limit of the estimate of total abundance is more than double the limit of 10,000 animals.
- The precision of estimates of abundance for each management unit and exclusion zone could potentially be further improved by additional or alternative stratification (e.g. habitat-based strata). More detailed maps of available tahr habitat across the PCL would be required to undertake this stratification.
- Further work should also investigate models of the relationship between tahr abundance and habitat characteristics. Such model-based estimates could provide more fine-scale resolution of the variation in tahr abundance across the PCL.

2 Introduction

Himalayan tahr (*Hemitragus jemlahicus*) were first introduced into New Zealand in 1904 and now occupy around 9600 km^2 of the Southern Alps (Cruz *et al.* 2017). After commercial harvesting reduced tahr populations by around 90% during the 1960's and 1970's, the population increased 6-fold following a moratorium on commercial harvesting in 1982 (Parkes 2009). Tahr are a declared wild animal under the "Wild Animal Control Act 1977", which provides provisions for the control of introduced wild animals to protect against their damaging effects on native vegetation, soils, water and other wildlife (Department of Conservation 1993). Tahr graze primarily on alpine tussock grassland (e.g. *Chionochloa* spp.) and caused widespread impacts on montane grasslands during the 1960's when their densities were high (Parkes 2009). However, impacts are still apparent at current population densities and tahr need to be controlled to lower densities to further reduce impacts on native vegetation (Cruz *et al.* 2017).

The Himalayan Tahr Control Plan (Department of Conservation 1993) defines intervention densities in terms of number of tahr per km^2 in each of seven management units (range: <1 to 2.5 tahr per km^2) and two exclusion zones (0 per km^2) (Table 1). However, insufficient monitoring data existed to estimate tahr abundances on these management units and exclusion zones. To address that knowledge gap, aerial surveys of tahr and other ungulates were conducted at 117 sites monitored as part of the national Biodiversity Monitoring and Reporting System (BMRS) (Allen *et al.* 2013) from 2016 to 2019. These data were then used to estimate the density and total abundance of Himalayan tahr on Public Conservation land (PCL) in each of the seven management units (MU) and two exclusion zones (EZ). This work updates a previous analysis that was based on the subset of 66 plots that were sampled from 2016 to 2018 (Ramsey & Forsyth 2018). We report results only for Himalayan tahr because this was the most abundant ungulate species and is the focus of active management by the Department of Conservation. Analysis of monitoring data for other ungulate species and from ungulate faecal pellet surveys will be the focus of a separate report.

3 Methods

3.1 Plot selection

The BMRS was developed to enable reporting on the status of native biodiversity and key threats (including pest animals) on New Zealand's Public Conservation Land by collecting data at plots at the vertices of an 8-km grid superimposed over New Zealand's Public Conservation Land (i.e. a spatially representative sampling network) (Allen *et al.* 2013). The origin of the grid was selected randomly. This design resulted in a total of 117 plots within PCL across the seven tahr management units and two exclusion zones (Table 1).

Monitoring was conducted at a randomly selected number of plots (without replacement) annually. During 2016, 16 plots were initially sampled with 22, 28 and 51 plots sampled in 2017, 2018 and 2019, respectively, giving 117 plots in total (Figure 1).

Table 1. The seven management units (MU) and two exclusion zones (EZ) defined in the Himalayan Tahr Control Plan (Department of Conservation 1993). 'Plots' is the number of 2 × 2 km plots on PCL that were subject to sampling from 2016 – 2019.

Unit/zone	Name	Intervention density (abundance)	Plots
MU1	South Rakaia/Upper Rangitata	2.5 km^2 (ca. 2000)	13
MU2	South Whitcombe Wanganui/Whataroa	2.0 km^2 (ca. 1500)	11
MU3	Gammack/Two Thumb	2.0 km^2 (ca. 3000)	17
MU4	Mount Cook/Westland National Parks Adjoining PCL on Liebig Range	<1.0 km^2 (ca. <500)	19
MU5	Ben Ohau	2.5 km^2 (ca. 1800)	8
MU6	Landsborough	1.5 km^2 (ca. 900)	11
MU7	Wills/Makarora/Hunter	<1.0 km^2 (ca. <100)	11
EZ1	North Rakaia/Mathais-North Whitcombe/Hokitika/Mungo	>0	10
EZ2	South of the Haast to Wanaka Highway	0	17

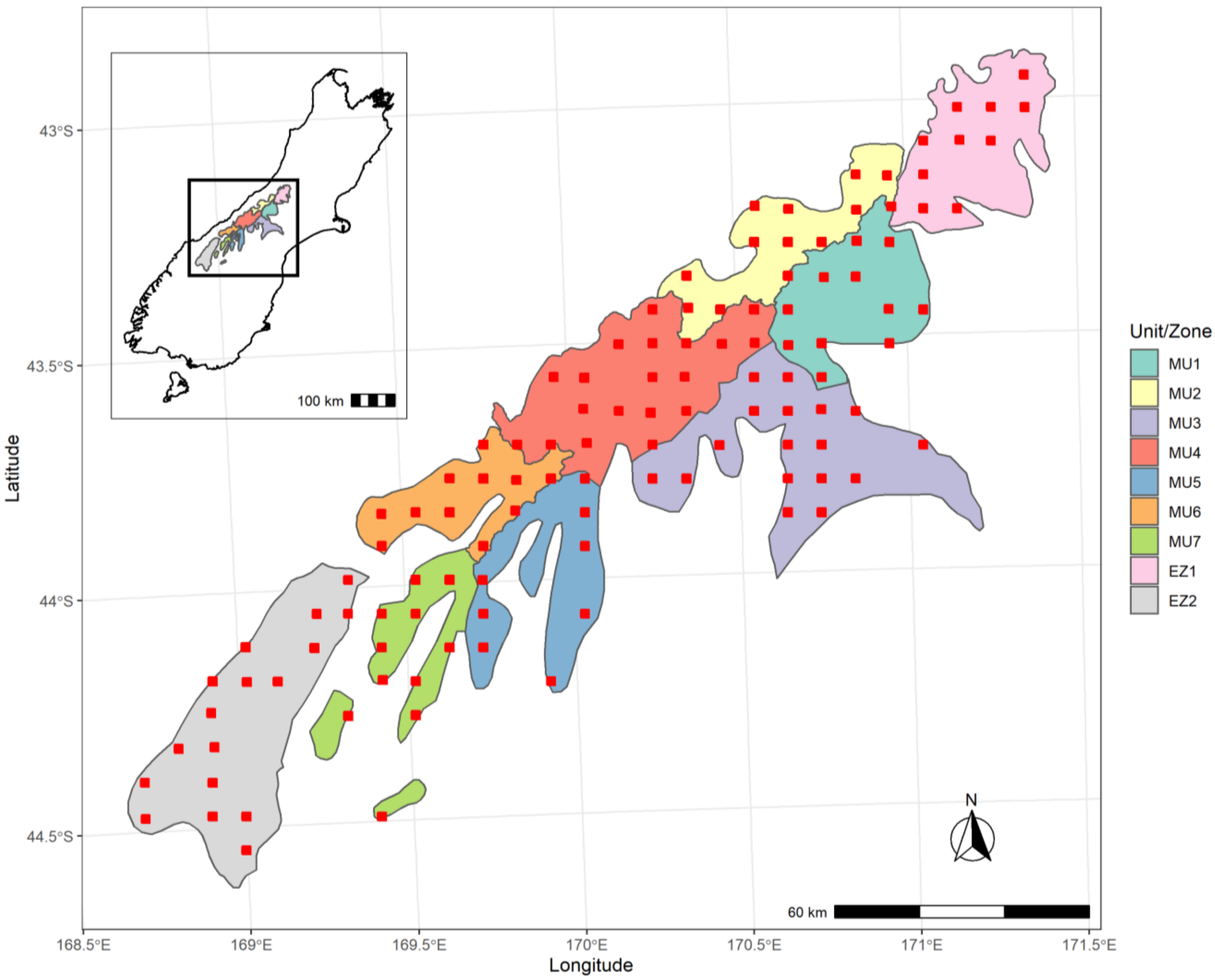

Figure 1. Location of the seven tahr management units (MU) and two exclusion zones (EZ) in the Southern Alps of New Zealand. Red squares show the locations of the 117 plots (2 x 2 km) where aerial surveys of tahr were undertaken.

3.2 Aerial survey protocol

The aerial survey protocol is described in detail elsewhere (Forsyth, Perry & McKay 2018 and references therein). Briefly, a 2 x 2 km plot was established at each site, with the centre of each plot being the vertex of the 8-km grid. Each 4 km^2 plot was subject to three separate counts undertaken from a helicopter (usually a Hughes 500D or Hughes 500E) at least 10 days apart. This interval between successive counts at a plot was chosen to minimise the disturbance effects of the helicopter on tahr in the subsequent two counts at that plot. Counts were undertaken during February–June (with most completed by May), well after the 30 November median birth date (Caughley 1971).

On each of the three sampling occasions the 4 km^2 plot was systematically flown by the helicopter flying at about 40–60 knots and at 20–70 m from the ground (depending on topography and wind). The pilot and one primary observer, seated next to the pilot, searched for tahr and other ungulates. When ungulates were sighted, the primary observer counted the individuals and assigned them to species (and sex-age classes where possible, but that information was not used in the analyses reported here). A recorder, seated in the rear behind the primary observer, recorded the locations and other details of each group.

3.3 Plot area

Although each plot was nominally 4 km^2 in area, this was the two-dimensional surface area of the plot. Due to the steep terrain on most plots, the actual surface area covered by each plot could be considerably greater than the nominal 4 km^2. Hence, to calculate the actual 3D surface area of each plot, each 2 x 2 km area was divided into 400 1-ha cells and the surface area of each cell calculated using a 15m digital Elevation Model (DEM). The 3D surface areas of each 1-ha cell were then added to give the 3D surface area for each plot. The 3D surface area was subsequently used for density calculations for each plot.

3.4 Abundance estimation

The total number of tahr counted within each plot, at each of the three sampling occasions, were used to estimate abundance corrected for imperfect detection using an *N*-mixture model for open populations (Dail & Madsen 2011). We assumed a simple exponential trend to model the changes in tahr abundance between successive sampling occasions (Humbert *et al.* 2009). Hence, the model was able to account for movement of tahr on or off the plot between the three sampling occasions. This model was the same as that used in Ramsey and Forsyth (2018). Further details of this model including summaries of model fit are provided in Appendix 1 (Figure A1).

For each plot, an estimate of average abundance was calculated as the mean of the estimates from the three sampling occasions. Tahr density for each plot was estimated similarly by dividing the abundance estimate by the three-dimensional area of each plot. To estimate the total abundance of tahr within each management unit / exclusion zone, we assumed that the sampled plots consisted of a stratified random sample of the total available plots that could have been sampled within PCL occurring in each management unit, with management units forming the strata. We assumed a two-stage sampling design where the overall estimate of abundance within each unit was composed of two sources of error, the spatial variation in tahr abundance among plots within each unit and the estimation error associated with the abundance estimate for each plot. Total abundance within each management unit was then estimated as the mean plot abundance in the unit multiplied by the total available plots within each unit. The total number of available plots within each unit was calculated by subdividing the two-dimensional area of PCL within the unit into all possible 2 x 2 km plots. The mean tahr density for each management unit was then calculated by dividing the estimated abundance for each management unit by the two-dimensional area of the management unit. Variance of the estimates of total tahr abundance and density within each management unit and overall abundance was calculated using finite sampling methods (Skalski 1994). More details on these calculations are provided in Appendix 2.

4 Results

4.1 Tahr density and abundance

The mean density of tahr (individuals/km^2) on each plot varied widely, from 0.02 to 37 (Figures 2 & 3). However, precision of some of the mean density estimates was low due to the changes in tahr density over the three sampling occasions at some plots (Figure A2, Appendix 3). The corresponding mean density of tahr within each management unit was also variable, ranging from 0.3 tahr/km^2 in MU7 to 10.8 tahr/km^{2}in MU5 (Table 2). The mean tahr densities exceeded the intervention densities specified in the Himalayan Thar Control Plan (Table 1) in all management units except MU7. Mean tahr densities in the two exclusion zones were 0.07 for EZ1 and 0.02 for EZ2, both above the intervention density of 0 (Table 2).

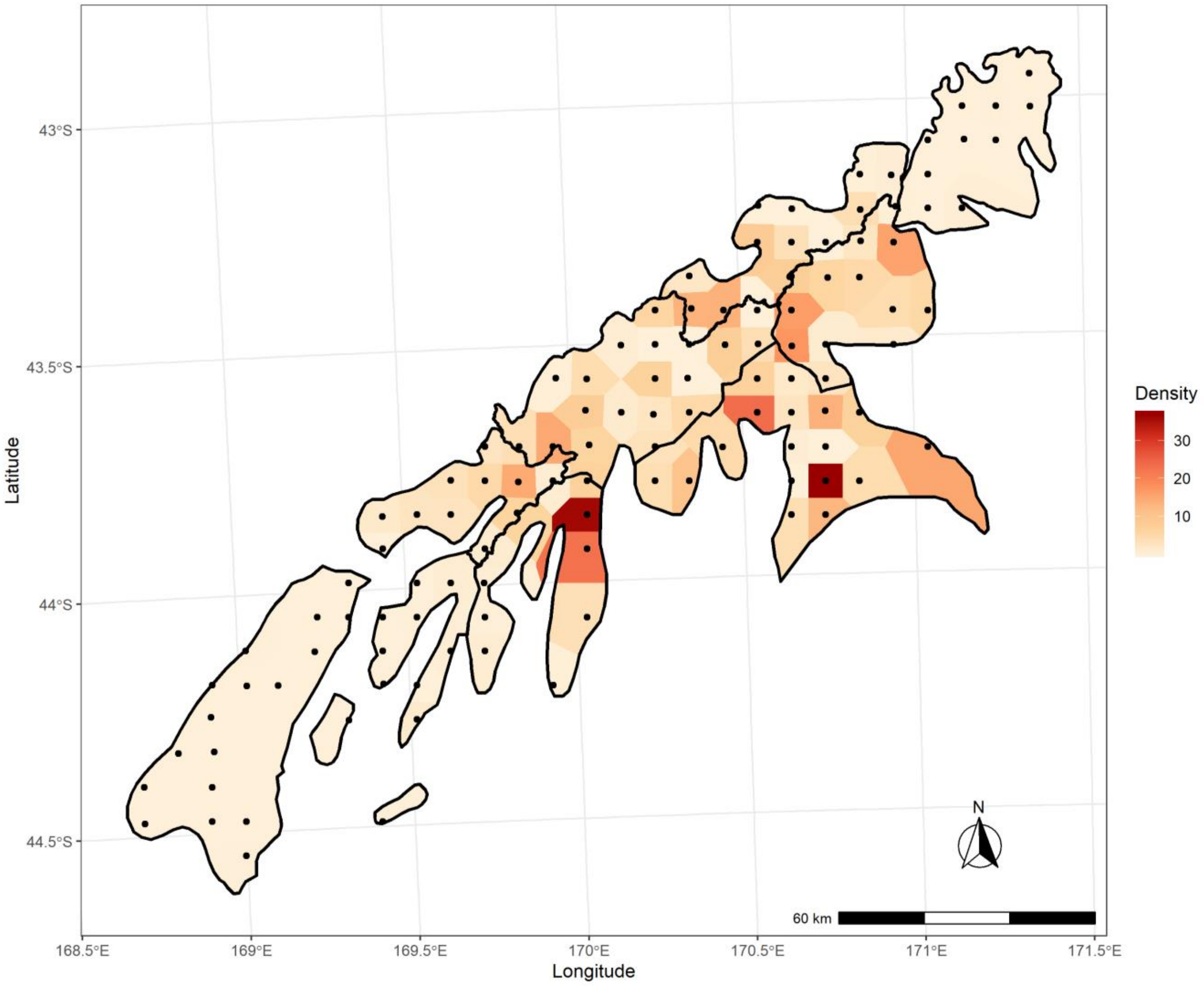

Figure 2. The average density of tahr (individuals/km²) on the area uniquely occupied by each of the 117 plots (black circles) sampled by aerial surveys from 2016 – 2019. The seven management units (MU) and two exclusion zones (EZ) are described in Table 1.

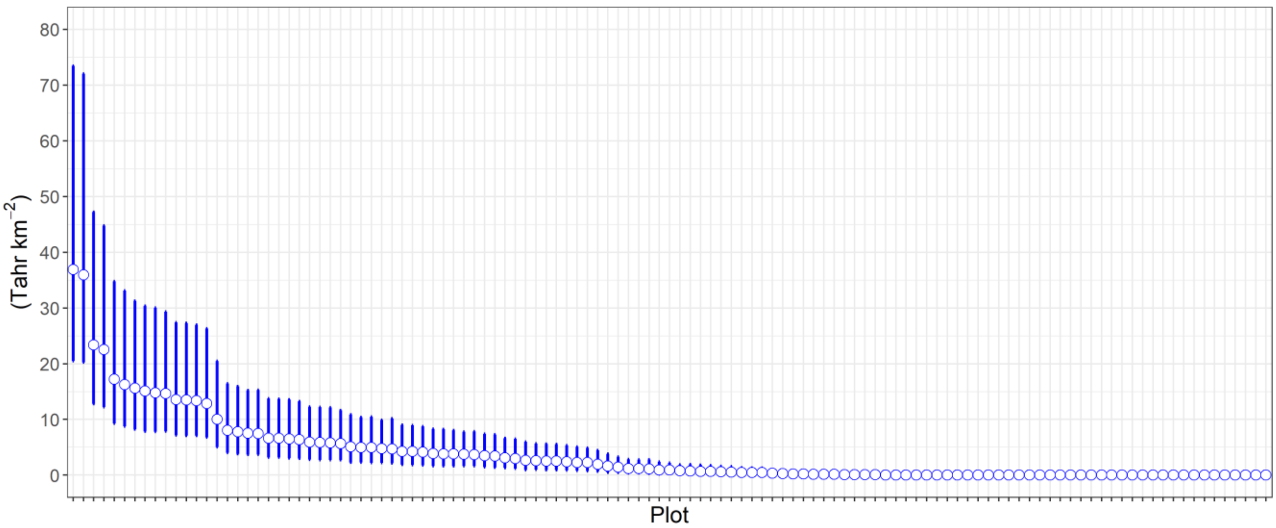

Figure 3. The estimates of average tahr density (open circles) and associated 95% credible intervals (solid lines) on each of the 117 plots sampled by aerial surveys from 2016 – 2019. The plots are shown in descending order of mean tahr density.

Table 2. Mean density of tahr (tahr/km^2) within each management unit and exclusion zone estimated from 117 plots subject to aerial surveys from 2016 – 2019. SD – standard deviation; LCL – lower 95% confidence limit; UCL – upper 95% confidence limit; *n* – number of plots. The seven management units (MU) and two exclusion zones (EZ) are described in Table 1.

Unit/Zone	Density	SD	LCL	UCL	*n*
MU1	8.1	2.1	4.8	13.4	13
MU2	5.3	2.1	2.5	11.3	11
MU3	10.0	2.7	6.0	16.9	17
MU4	4.7	1.1	3.0	7.3	19
MU5	10.8	5.7	3.8	30.3	8
MU6	4.6	1.6	2.3	9.1	11
MU7	0.3	0.1	0.1	0.7	11
EZ1	0.07	0.05	0.02	0.29	10
EZ2	0.02	0.01	0.01	0.04	17

The estimated total abundance of tahr within management units and exclusion zones ranged from 169 individuals in MU7 to 8,663 tahr in MU3 (Table 3, Figure 4). Abundance in the two exclusion zones was estimated to be around 30 – 50 individuals (Table 3, Figure 4). In general, the precision of the abundance estimates for individual management units has improved slightly on the estimates in Ramsey and Forsyth (2018) with the addition of the 51 plots sampled in 2019. However, precision of estimates for some units still remains low (e.g. MU5 had 95% confidence intervals of 1,757 – 13,951 tahr). This was a consequence of the high spatial variation in tahr density among plots as well as the comparatively small number of sampled plots for these units.

The total abundance of tahr on PCL was estimated to be 34,478 (95% confidence interval; 26,522 – 44,821) (Table 4). This estimate is almost identical to that given in Ramsey and Forsyth (2018) using data from the subset of 66 plots sampled from 2016 to 2018. The precision of the overall abundance estimate has, however, improved slightly from a coefficient of variation (CV) of 17% (Ramsey & Forsyth 2018) to 13% (Table 4).

Table 3. Estimates of total abundance (*N*) of tahr within each management unit and exclusion zone based on monitoring data from 117 plots subject to aerial surveys from 2016 – 2019. SD - standard deviation; LCL - lower 95% confidence limit; UCL - upper 95% confidence limit; *u* - number of sampled plots; *U* - estimated number of plots available to be sampled.

MU	*N*	SD	LCL	UCL	*u*	*U*
MU1	6182	1601	3721	10269	13	192
MU2	4357	1694	2033	9335	11	207
MU3	8663	2306	5142	14596	17	216
MU4	6973	1582	4470	10879	19	371
MU5	4950	2617	1757	13951	8	115
MU6	3096	1091	1552	6176	11	170
MU7	169	82	65	438	11	152
EZ1	54	39	13	225	10	197
EZ2	34	13	16	73	17	408

Table 4. Estimated total abundance (*N*) of tahr across the PCL from 2016 – 2019. SD – standard deviation; CV – % coefficient of variation; LCL – lower 95% confidence limit; UCL – upper 95% confidence limit.

N	SD	CV	LCL	UCL
34,478	4615	13	26,522	44,821

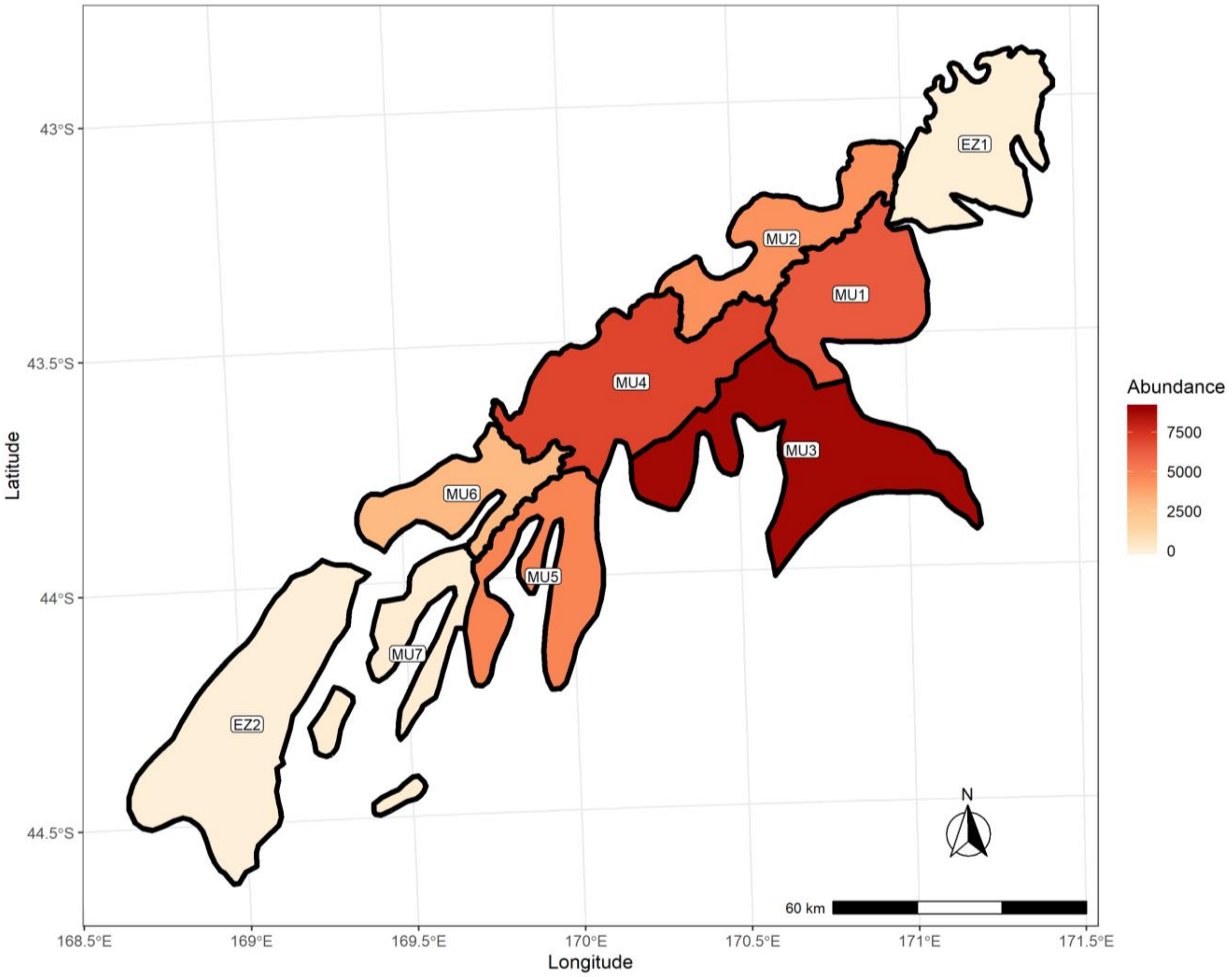

Figure 4. The total abundance of Himalayan tahr within each management unit and exclusion zone based on monitoring data from 117 plots subject to aerial surveys from 2016 – 2019.

5 Discussion

The Himalayan Thar Control Plan identified a “population of 10,000 over the entire range as a presently acceptable maximum” (Department of Conservation 1993: 2). The estimated tahr population reported here is only for the PCL, which is approximately 62% of the tahr breeding range as defined in Department of Conservation (1993). Hence, the total tahr population across the entire breeding range is likely much greater than estimated here. The tahr population on PCL (Table 4) clearly exceeds the 10,000 specified for the entire tahr range, with the lower 95% confidence limit more than double that value.

Tahr densities were highly variable across the seven tahr management units. Average tahr densities exceeded the thresholds defined in the Himalayan Tahr Control Plan (Department of Conservation 1993; Table 1) for all management units except MU7. Average tahr densities also exceeded zero in both exclusion zones. Despite additional monitoring data from 51 plots sampled in 2019, there was still high uncertainty around the estimated density of tahr for some management units. This uncertainty was due to high spatial variation in tahr density among plots within the management unit and the small number of plots sampled in some units. For example, tahr density on plots within MU5 ranged from an average of 0.1 to 35 tahr/km^2. High spatial variation in tahr densities among plots within MU were a general feature of the data with 32% of plots recording zero counts of tahr.

The precision (coefficient of variation) of the tahr abundance estimates for each management unit and exclusion zone improved with the addition of the monitoring data from 2019. However, the improvement in precision was not as large as might be expected given that an extra 51 plots were added to the 66 plots sampled up to 2018. Hence, the marginal gain from increasing sample size to improve the precision of abundance estimates for future monitoring of tahr should be subject to further investigation. As there were insufficient numbers of plots sampled per year to enable annual density estimates for each management unit, our estimate of overall abundance necessarily combined plots sampled in different years. Hence, our estimates for each management unit effectively averages over any interannual changes in abundance that may have occurred. However, estimates of total abundance of tahr have remained consistent as additional monitored plots have been added over the four-year sampling period. Indeed, the overall estimate of abundance from the first two years monitoring data (35,633) (Ramsey 2018) was similar to the current estimate after four years data collection (34,478). Once data become available for additional rounds of monitoring for each plot, an in-depth analysis of population trends in each management unit can be undertaken.

The precision of estimates of abundance for each management unit and exclusion zone could potentially be further improved by additional or alternative stratification (e.g. habitat-based strata). More detailed maps of available tahr habitat across the PCL would be required to undertake this stratification. Further work is also being undertaken to investigate models of the relationship between tahr abundance and habitat variables. Such model-based estimates could also provide an alternative means to more accurately map the distribution of tahr across each management area.

6 References

Allen, R.B., Wright, E.F., Macleod, C.J., Bellingham, P.J., Forsyth, D.M., Mason, N.W.H., Gormley, A.M., Marberg, A.E., Mackenzie, D.I. & McKay, M. (2013) *Designing an Inventory and Monitoring Programme for the Department of Conservation's Natural Heritage Management System*. Landcare Research Contract Report LC1730, Landcare Research, Lincoln, New Zealand.

Brooks, S. & Gelman, A. (1998) General methods for monitoring convergence of iterative simulations. *Journal of Computational and Graphical Statistics*, **7**, 434–455.

Carpenter, B., Gelman, A., Hoffman, M.D., Lee, D., Goodrich, B., Betancourt, M., Brubaker, M., Guo, J., Li, P. & Riddell, A. (2017) *Stan* : A Probabilistic Programming Language. *Journal of Statistical Software*, **76**, 1–32.

Caughley, G. (1971) The season of births for Northern-Hemisphere ungulates in New Zealand. *Mammalia*, **35**, 204–219.

Cruz, J., Thomson, C., Parkes, J.P., Gruner, I. & Forsyth, D.M. (2017) Long-term impacts of an introduced ungulate in native grasslands: Himalayan tahr (*Hemitragus jemlahicus*) in New Zealand's Southern Alps. *Biological Invasions*, **19**, 339–349.

Dail, D. & Madsen, L. (2011) Models for estimating abundance from repeated counts of an open metapopulation. *Biometrics*, **67**, 577–587.

Department of Conservation. (1993) *Himalayan Thar Control Plan*. Canterbury Conservancy Conservation Management Series No. 3, Department of Conservation, Christchurch, New Zealand.

Forsyth, D.M., Perry, M. & McKay, M. (2018) *Field Protocols for Tier 1 Monitoring: Himalayan Tahr Abundance Monitoring Protocol Version 2.0.* Department of Conservation Document DOC-2650377, Department of Conservation, Wellington.

Gelman, A., Meng, X.L. & Stern, H. (1996) Posterior predictive assessment of model fitness via realized discrepancies. *Statistica Sinica*, **6**, 733–807.

Humbert, J.Y., Scott Mills, L., Horne, J.S. & Dennis, B. (2009) A better way to estimate population trends. *Oikos*, **118**, 1940–1946.

Parkes, J.P. (2009) Management of Himalayan thar (*Hemitragus jemlahicus*) in New Zealand: The influence of Graeme Caughley. *Wildlife Research*, **36**, 41–47.

Ramsey, D.S.L. (2018) *Tahr Density Estimates from Aerial Surveys - Preliminary Results*. Unpublished report to the Department of Conservation, New Zealand, https://www.doc.govt.nz/globalassets/documents/parks-and-recreation/hunting/west-coast/tahr-density-estimates.pdf.

Ramsey, D.S.L. & Forsyth, D.M. (2018) *Estimates of Himalayan Tahr (Hemitragus Jemlahicus) Abundance in New Zealand: Results from Aerial Surveys*. Unpublished report to the Department of Conservation, New Zealand.

Skalski, J.R. (1994) Estimating wildlife populations based on incomplete area surveys. *Wildlife Society Bulletin*, **22**, 192–203.

Thompson, S.K. (1992) *Sampling*. John Wiley & Sons, New York.

Thompson, W.L., White, G.C. & Gowan, C. (1998) *Monitoring Vertebrate Populations*, 1st ed. Academic Press.

Appendix 1

Abundance model

The counts of tahr at each plot, at each time period, were used to estimate abundance corrected for imperfect detection using an N-mixture model for open populations (Dail & Madsen 2011). We treated each of the three replicate counts at each plot as potentially being open to movement (immigration/emigration) between sampling times. Hence, tahr abundance at each plot i and sampling period t (t = 1, 2, 3) was modeled as

$$y_{it} \sim Bin(p, N_{i,t})$$

where $N_{i,i}$ is the abundance of tahr in each plot i during sampling occasion t and p is the detection probability of tahr during aerial surveys. In order to estimate abundance $N_{i,t}$ at each sampling period t, it is assumed that abundance follows a first order Markov process where abundance at time t was dependent on the abundance at time t-1, using an exponential trend model as follows

$$N_{i,t} \sim Poisson(\lambda_{i,t})$$
$$\log(\lambda_{i,1}) = \eta_i$$
$$\log(\lambda_{i,t}) = \log(\lambda_{i,t-1}) + r_i T_{i,t-1}$$
$$\operatorname{logit}(p) = \phi$$
$$r_i \sim N(\mu_r, \sigma_r)$$
$$\eta_i \sim N(0, 5)$$
$$\mu_r \sim N(0, 1)$$
$$\sigma_r \sim t_4(0, 1)$$
$$\phi \sim N(0, 1.6)$$

where r_i was the change in the (log) population size at each between period $t-1$ and t for plot i and $T_{i,t}$ was the time period (weeks) between sampling periods for each plot (Humbert *et al.* 2009; Dail & Madsen 2011). The N-mixture open population model above was fitted in a Bayesian framework using Hamiltonian Markov Chain Monte Carlo (HMCMC) sampling using `Stan ver.2.18.2` (Carpenter *et al.* 2017). The rate of change parameters for each plot (r_i) were modeled with a hierarchical prior distribution specified as $N(\mu_r, \sigma_r)$. Weakly informative prior distributions were placed on the initial log population abundance for each plot, $\eta \sim N(0, 5)$ as well as the hyperparameters, $\mu_r \sim N(0, 5)$, $\sigma_r \sim t_4(0, 1)$, $\phi \sim N(0, 1.6)$. The model was updated for 6000 iterations using 3 chains with the first 1000 iterations used as a burn-in and discarded leaving 15,000 samples to form the posterior distribution of each parameter.

Following updating, the posterior distribution of the parameters were judged to have converged based on visual inspection of traceplots and estimates of the Brooks-Gelman-Rubin convergence criterion $\hat{R}$ (Brooks & Gelman 1998) all having values <1.01. Posterior predictive checks (Gelman, Meng & Stern 1996) were undertaken by comparing predictions of the counts of tahr on each plot under the model with the observed counts of tahr. We performed posterior predictive checks for four summary statistics, the proportion of plots with zero counts, the mean count, the standard deviation of the counts and the maximum count. All counts (observed and predicted) were first summed over the three occasions to give the total count of tahr on each plot. In each case, the distribution of the summary statistics for the predicted counts were a close match to the summary statistics for the observed counts (Figure A1).

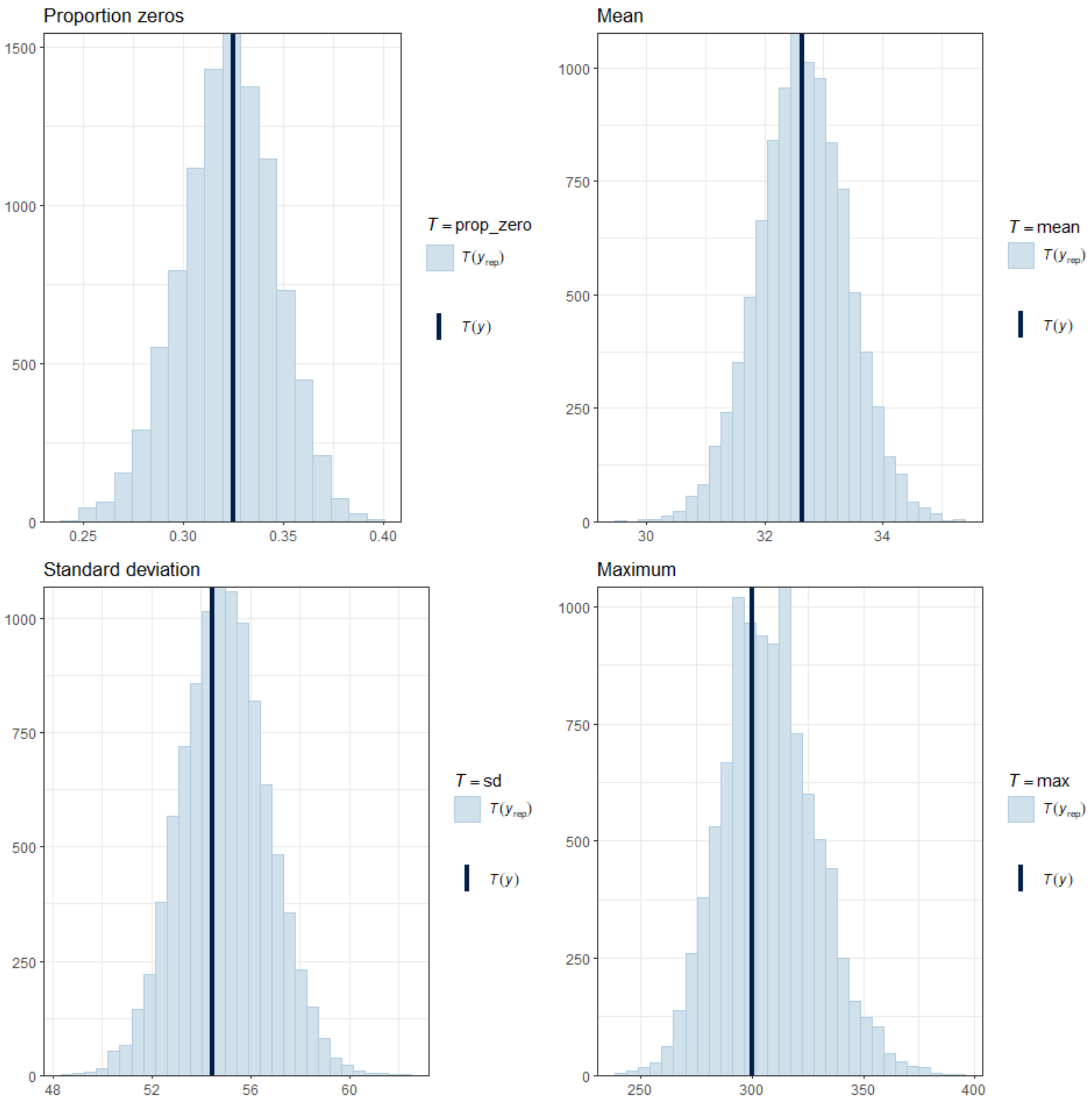

Figure A1. Posterior predictive checks comparing summary statistics (*T*) of the predicted counts of tahr under the model, with the observed counts of tahr on each plot. Summary statistics are the proportion of plots with zero counts, the mean total count, the standard deviation of the total count and the maximum total count. Total counts for each plot were calculated by summing the per-occasion counts. Pale-blue histograms give the distribution of the summary statistic predicted by the model $T(y_{rep})$ and dark-blue bars give the summary statistic for the observed counts $T(y)$.

Appendix 2

Abundance estimates for each management unit and exclusion zone

We used finite sampling estimators assuming a stratified random sampling design (Thompson 1992; Skalski 1994; Thompson, White & Gowan 1998) to estimate total abundance within each stratum, based on incomplete surveys. Here, management units correspond to strata. If u number of plots are sampled from a total number U in stratum h, the estimate of abundance is given by

$$\widehat{N_h} = \overline{N_h} U_h$$

where $\widehat{N_h}$ is the estimate of total abundance for stratum h, $\overline{N_h}$ is the mean abundance over the u plots and U_h is total number of plots in stratum h. The estimate of variance is given by

$$\widehat{Var}(\widehat{N_h}) = U_h^2\{(1 - \frac{u_h}{U_h}) \frac{\hat{S}_{N_{hi}}^2}{u_h} + \frac{\overline{\widehat{Var}(\widehat{N_{hi}|N_{hi}})}}{U_h}\}$$

where

$$\hat{S}_{N_{hi}}^2 = \frac{\sum_{k=1}^{u} (\widehat{N}_{hi} - \widehat{\overline{N_h}})^2}{u_h - 1}$$

and

$$\overline{\widehat{Var}(\widehat{N_{hi}}|N_{hi})} = \frac{\sum_{k=1}^{u_h} \widehat{Var}\,(\widehat{N_{hi}}|N_{hi})}{u_h}$$

The total abundance over all sampled management units is then simply

$$\sum_{h=1}^{n} \widehat{N_h}$$

with variance

$$\sum_{h=1}^{n} \widehat{Var}\,(\widehat{N_h})$$

An estimate of the average density in each management unit can also be calculated as

$$\widehat{D_h} = \frac{\widehat{N_h}}{A_h}$$

Where A_h is the (2 dimensional) area of management unit h. This has variance of

$$\widehat{Var}(\widehat{D}_h) = \frac{\widehat{Var}(\widehat{N_h})}{A_h^2}$$

Appendix 3

Figure A2. The estimates of tahr density on each of the three sampling occasions for each of the 117 sampled plots (open circles and lines). Black solid circles are the naïve estimates of tahr density calculated from the raw counts. For each plot, the range for the y-axis is scaled to the range of the data. The alpha-numeric (e.g., AA144) is the unique plot identifier.